Enhanced Soft X-ray Reflectivity of Cr/Sc Multilayers by Ion Assisted Sputter Deposition

F. Eriksson,[a] G. A. Johansson,[b] H. M. Hertz,[b] and J. Birch[a]
[a]Thin Film Division, Department of Physics, Linköping University, S-58183 Linköping, Sweden
[b]Biomedical and X-ray Physics, Royal Institute of Technology, S-10044 Stockholm, Sweden

ABSTRACT

Cr/Sc multilayers have been grown on Si substrates using DC magnetron sputtering. The multilayers are intended as condenser mirrors in a soft x-ray microscope operating at the wavelength 3.374 nm. They were designed for normal reflection of the first and second order with multilayer periods of 1.692 nm and 3.381 nm, and layer thickness ratios of 0.471 and 0.237, respectively. At-wavelength soft x-ray reflectivity measurements were carried out using a reflectometer with a compact soft x-ray laser-plasma source. The multilayers were irradiated during growth with Ar ions, varying both in energy (9-113 eV) and flux, in order to stimulate the ad-atom mobility and improve the interface flatness. It was found that to obtain a maximum soft x-ray reflectivity with a low flux (Cr=0.76, Sc=2.5) of Ar ions a rather high energy of 53 eV was required. Such energy also caused intermixing of the layers. By the use of a solenoid surrounding the substrate, the arriving ion-to-metal flux ratio could be increased 10 times and the ion energy could be decreased. A high flux (Cr=7.1, Sc=23.1) of low energy (9 eV) Ar ions founded the most favourable growth condition in order to limit the intermixing with a subsistent surface flatness.

Keywords: Cr/Sc, multilayer, reflectivity, ion assisted sputter deposition, ion energy, ion flux, soft x-ray microscopy, water-window

1. INTRODUCTION

Multilayer x-ray optics have many useful applications such as x-ray microscopy,[1,2] x-ray astronomy,[3,4] x-ray lithography,[5] x-ray microanalysis.[6] In particular, multilayer mirrors for the water window region (λ=2.2–4.4 nm) has an important application when used as optical elements in microscopy of biological specimens, due to the large absorption contrast between protein and water. In soft x-ray microscopy using a laser-plasma line source a multilayer mirror is needed as a condenser to focus the x-rays on the specimen.[7] A primary goal is to maximize the normal incidence reflectance. To achieve optimum performance it requires that the multilayer period and layer thickness ratio are optimized to add, coherently and in phase, the reflected amplitudes from each interface.

It is known that interfacial roughness leads to a loss of specular reflectivity which is detrimental for the optical properties.[8,9] Since the normal incidence reflectivity, R, for a given x-ray wavelength, λ, of a multilayer is greatly influenced by the ratio between the interface roughness, σ, and the multilayer period, Λ, according to the Debye-Waller-like factor, $\exp[-(2\pi m\sigma/\Lambda)^2]$, the absolute value of the interface roughness becomes more important at small multilayer periods.[10,11] E.g., model calculations predicts that for a semi-infinite Cr/Sc multilayer a decrease in interface roughness from 0.5 nm to 0.3 nm for the wavelength λ=3.374 nm in a multilayer with period Λ=1.692 nm theoretically corresponds to an increase in reflectivity from $R=0.032R_0$ to $R=0.289R_0$. Therefore it is important to achieve as smooth and compositionally abrupt interfaces as possible when depositing multilayer x-ray mirrors.

In multilayer mirrors the effects of imperfect interfaces such as intermixing and roughness will be enhanced due to the large amount of interfaces contributing to the reflectance. There are mainly two different processes in the multilayer growth that causes the interface chemical composition profile to broaden, namely interdiffusion and intermixing. Interdiffusion is thermally activated transport of material across the interface, and intermixing is related to the mixing of the interfaces due to energetic particle bombardment. Both leads to a larger interface concentration gradient, i.e. a larger interface width, and they have the same influence on the reflectivity, although they originate from physically different effects. A low substrate temperature and no energetic particle irradiation during growth will minimize interdiffusion and interface mixing. However, such conditions may lead to a kinematically limited growth with an increased and accumulated roughness as a consequence.[12,13] On the other hand, increasing the substrate temperature, in order to increase the ad-atom mobility and hence reduce accumulated roughness, may activate bulk diffusion across the interfaces.[14] An appearent increase of the surface temperature, achieved by ion irradiation during growth, will enhance ad-atom mobility while heating of the bulk multilayer is avoided. Such conditions have been demonstrated to reduce the accumulated roughness[15] although on the expense of interface abruptness due to intermixing[16] of the interfaces. Post deposition grazing incidence ion irradiation has also proven to smoothen the layers leading to significant improved reflectivities.[17,18] Also other effects such as resputtering and defect creation have been observed.[19] It is expected that an increased flux of ions with lower energy would counteract for the intermixing, while the positive effects of the enhanced

Soft X-Ray and EUV Imaging Systems II, Daniel A. Tichenor, James A. Folta, Editors,
Proceedings of SPIE Vol. 4506 (2001) © 2001 SPIE · 0277-786X/01/$15.00

ad-atom mobility is subsistent. A variety of plasma based deposition techniques exists that might be used for ion assisted deposition.[20]

In this work Cr/Sc multilayers have intentionally been irradiated during magnetron sputter deposition with Ar ions of different energies (E) and different ion-to-metal flux ratios (Φ). Ions, extracted from the plasma and accelerated to kinetic energies in the range of 9-113 eV through a negative substrate bias, have been utilized in order to stimulate the ad-atom mobility and improve the interface flatness. The flux of ions was controlled by the use of a solenoid surrounding the substrate, which extracts energetic secondary electrons from the target region towards the vicinity of the substrate where they increase the plasma density by ionization. By synchronizing both the magnitude and direction of the solenoid current with the deposition from each magnetron, the magnetic field of the solenoid was coupled with the magnetic field of the magnetron used for deposition and the ion flux density on the substrate could thus be set independently for deposition from each magnetron.

This is an easy way to change and control the plasma growth conditions in a broad region, such that both ion current density and ion energy at the substrate surface can be varied individually for the two deposited materials.

2. EXPERIMENTAL DETAILS

The multilayers were deposited on chemically cleaned (10 min ultrasonic cleaning in each of trichlorethylene, acetone and isopropanol) Si (100) substrates with a native oxide using a dual DC magnetron sputtering system (Figure 1). The size of the chamber is 500 mm in diameter and 350 mm in height, and the target to substrate distance is 120 mm. A background pressure of about $2 \cdot 10^{-7}$ Torr ($2.67 \cdot 10^{-5}$ Pa) is obtained using a turbo molecular pump backed by a rotary vane pump. The two 75 mm diameter magnetrons are placed in the top of the chamber with a tilt angle of 25° against the substrate table normal. The configuration of the magnets in the magnetrons is such that the outer magnetic field lines are positively coupled to each other, guiding secondary electrons away from the cathodes towards the substrate, and thus extending the plasma to the substrate region. Between the magnetrons an electrically isolated μ-metal shield prevents cross-contamination and force the magnetic field lines to connect beneath the shield closer to the substrate. Ar gas, 99.9997 %, was introduced to a working sputtering gas pressure of 3 mTorr, as measured with a capacitance manometer.

The target discharges were established with constant-current power supplies and discharge currents (voltages) of 0.060 A (-255 V) and 0.060 A (-280 V) were used for the Sc (99.9 %) and Cr (99.94 %) target, respectively. This yielded Sc and Cr deposition rates of about 0.025 nm/s and 0.035 nm/s. Both magnetrons were running continously during the deposition, and the material fluxes to the substrate were regulated by fast acting computer controlled shutters located in front of the magnetrons.

The deposition rates were determined by growing two multilayers with different Cr/Sc layer thickness ratios, with known layer deposition times. The multilayer period was then calculated from the position of the multilayer peaks in a low-angle hard x-ray reflectivity pattern. This yields an equation system from which the deposition rates can be extracted using Cramers rule.[21]

The substrates (40x20x0.5 mm^3) were mounted on a rotating substrate table, rotating with a constant rate of 60 rpm, directly in line of sight of both magnetrons. The substrate table was electrically isolated from the system and a negative bias voltage could be applied to the substrate in order to attract Ar-ions from the plasma.

By the use of a solenoid surrounding the substrate, and choosing the direction of the current properly, the magnetic field from either one of the magnetrons could be coupled to the magnetic field of the solenoid. Solenoid currents of 0 A and 5 A were utilized in order to study the influence of different fluxes of ions to the substrate. Shown in Figure 2 are two photographs of the plasma with a solenoid current of 0 A and 5 A, respectively. The solenoid was made of capton insulated Cu wire (ϕ=2 mm) wound about 220 turns on a cylindrical stainless-steel frame with an inner diameter of 125 mm. A detailed characterization of this experimental setup is given in reference 22.

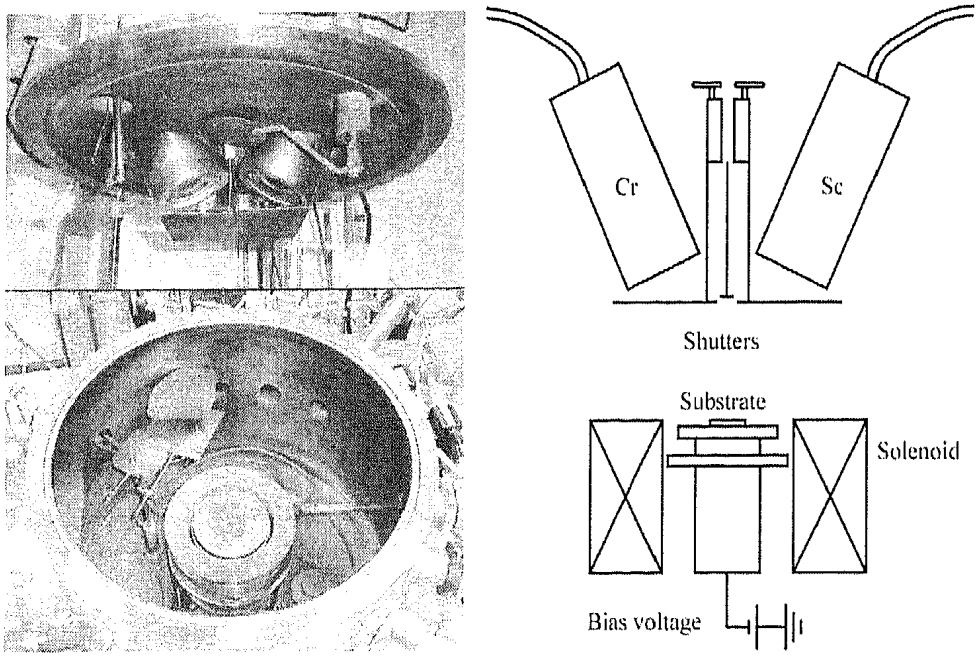

Figure 1: Dual DC magnetron sputtering system, showing magnetrons, computer controlled-shutters, rotating substrate table and surrounding solenoid.

Electrical probe measurements were performed to determine the plasma characteristics and the effects of the solenoid. To be able to measure both in the electron-current region, as well as in the ion-current region, two different probe geometries were used. A Langmuir probe, a 4 mm long tungsten wire with 0.15 mm radius was used to determine the floating potential and the plasma potential. The kinetic energy of the Ar ions is then simply obtained as the difference between the plasma potential and the applied bias voltage, since the mean free path of the Ar ions (several cm) is much larger than the dark sheath above the substrate (less than a mm). For the ion current density measurements a flat probe of stainless-steel, 15 mm in diameter, was used. The probe was surrounded by a flat stainless-steel shield with the same potential as the probe, in order to prevent edge effects to influence the effective collecting probe surface. Data collection was made by sweeping the bias voltage and simultaneously measure the probe current. From these data the ion-to-metal flux ratios, Φ, could be determined. Both probes were positioned at the substrate holder in the focal point of the magnetrons.

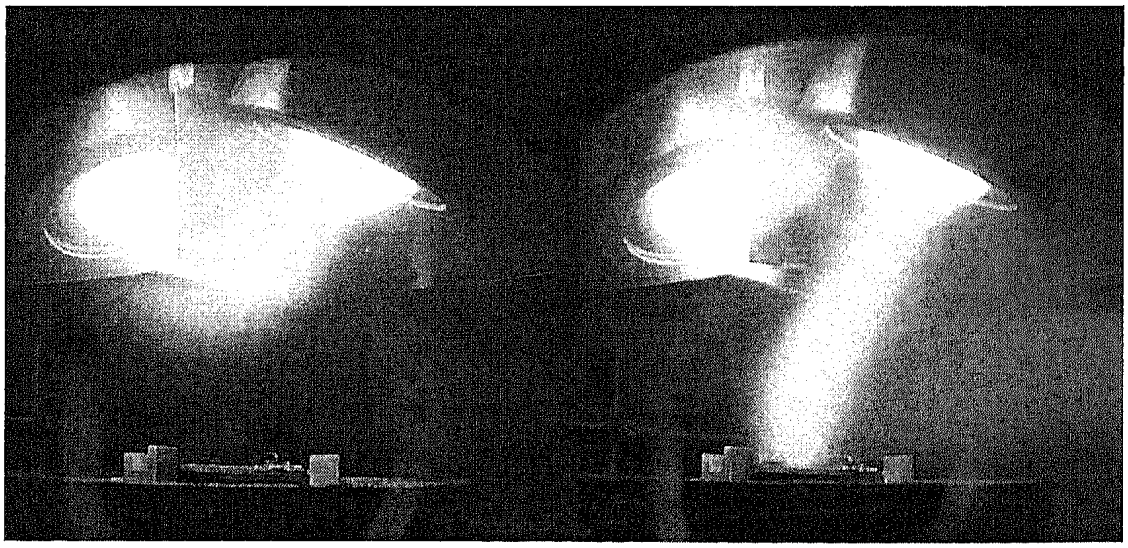

Figure 2: Photograph of the plasma with a solenoid current of 0 A to the left and 5 A to the right. Secondary electrons ejected from the target are guided towards the substrate and the plasma density is clearly enhanced in the substrate region when the solenoid is used.

Nanostructural properties of the multilayer structures were obtained from hard x-ray low-angle reflectivity measurements, using a Philips PW1710 powder diffractometer with a copper anode source (Cu K_α, λ=1.54 Å), operating at 0.8 kW and with an accuracy of 0.015° 2θ. A 2.5 s counting time was used at each 2θ increment of 0.005°. The Cu K_β-radiation was attenuated by a Ni-filter between the source and the sample. Directly after the x-ray source a 0.25°

divergence slit and a 2 mm wide brass mask was used to collimate the beam and to limit the size of the x-ray beam on the sample. In front of the detector a 0.1 mm antiscatter slit and a 0.25° divergence slit followed by a curved Ge-crystal monochromator was used. The diffractometer had decoupled detector (2θ) and sample (ω) axes so that coupled ω-2θ scans as well as ω-rocking curves could be performed. The intensity was detected with a proportional Xe-gas filled detector.

Specular hard x-ray reflectivity measurements from 0.7°-20° 2θ were performed on all samples. From these the multilayer period were calculated from the position of the Bragg reflections. Individual layer thicknesses and interface widths were determined by fitting model calculations of the specular reflectivity to the experimental data using the Wingixa software from Philips. Non-specular transverse ω-rocking scans for constant 2θ-values, corresponding to the first Bragg peak reflection of the investigated multilayers were also performed. These scans reveal how much of the x-rays that are specularly reflected and diffusively scattered, and hence gives qualitative information about the interface roughness.

The near-normal at-wavelength reflectivity of the multilayers was investigated using a soft x-ray reflectometer operating at the same wavelength as the microscope for which the mirrors are designed.[23,7] The reflectometer is based on a high-brightness line-emitting laser-plasma source utilizing an ethanol liquid-jet target emitting mainly λ=3.374 nm corresponding to the carbon VI line. By using a multilayer with known absolute reflectivity, as a calibration standard, absolute reflectivity up to 85° grazing incidence angle was measured. The detector system consists of two soft x-ray photodiodes, one for measuring the reflected x-rays and the other for monitoring the source intensity. The reference sample, a Cr/Sc multilayer with 100 bilayers and a period of 3.468 nm, was measured at Calibration and standards beamline 6.3.2 at the Advanced Light Source. The reflectivity of the reference sample was 10 % at 29.3° and 0.4 % at 78.5° for the first and second order reflectivity, respectively. By performing comparative measurements with the reference multilayer it is possible to measure the absolute reflectivity of other samples.

To determine the optimal design of the multilayers, i.e. the period, the layer thickness ratio and the total number of bilayers, for maximal reflectivity, calculations using the IMD code[24] was utilized. This yielded a multilayer period of Λ=1.692 nm and a layer thickness ratio of $\Gamma=d_{Cr}/\Lambda$=0.471 for multilayers designed for the first order normal reflection, and Λ=3.381 nm and Γ=0.237 for the second order. Using the same code it was predicted that 90 % of the expected theoretical reflectivities from semi-infinite multilayer stacks (35 % for Λ=1.692 nm and 23 % for Λ=3.381 nm) should be achieved with about 300 bilayers of Λ=1.692 nm and 270 bilayers of Λ=3.381 nm. However, since the reflectometer only can perform measurements up to grazing incidence angles of 85° the multilayer period, aimed for at the depositions, was slightly larger, about Λ=1.75 nm and Λ=3.5 nm for the first and second order, respectively.

3. RESULTS AND DISCUSSION

From electrical probe measurements it was found that the ion-to-metal flux ratios were Φ_{Cr}=0.76 and Φ_{Sc}=2.5 without the solenoid. When changing the solenoid current from 0 A to 5 A the ratios increased about 10 times for both Cr and Sc to Φ_{Cr}=7.1 and Φ_{Sc}=23.1, respectively. The plasma potential did not vary between Cr and Sc deposition, but it decreased by 14 V from 8.0 V to -6.1 V, when the solenoid current was increased. Thus, the energy of the ions, $E_{ion}=|V_p-V_s|$ eV, attracted by the substrate is 8.0 eV higher and 6.1 eV lower than that indicated by the substrate bias potential when the coil is off and on, respectively. The floating potentials, V_f, were the same for both Cr and Sc and were determined to V_f =-15 V and V_f =-4 V with and without the use of the solenoid. This shows that considerably more secondary electrons are guided towards the substrate when a magnetron is coupling to the solenoid, and consequently more ionized Ar will be available in the vicinity of the substrate. This in turn means that a lower bias voltage is required to attract a larger amount Ar ions from the plasma, permitting ion-stimulated ad-atom mobility using very low energy ions to reduce intermixing effects.

To study the effects of different deposition ion energies for solenoid currents of 0 A and 5 A, i.e. using low (Φ_{Cr}=0.76, Φ_{Sc}=2.5) and high (Φ_{Cr}=7.1, Φ_{Sc}=23.1) fluxes of Ar ions at the sample, hard x-ray Cu-Kα reflectivity measurements were performed on the multilayers grown with different ion energies.

Figure 3 shows a hard x-ray reflectivity curve together with a simulation. The multilayer, which was designed for the second order reflection of λ=3.374 nm, contains 20 bilayers and was deposited using a high Ar ion flux with an energy of 24 eV.

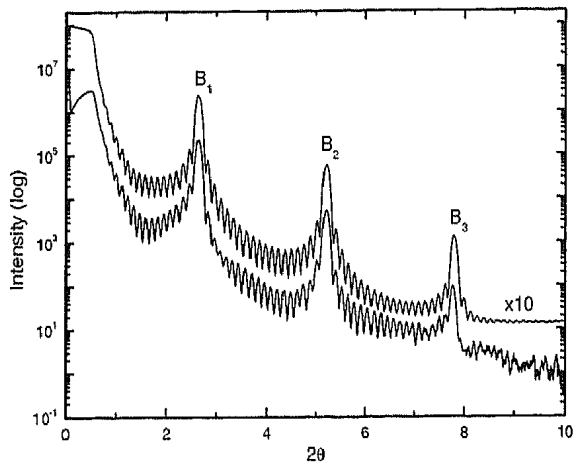

Figure 3: Hard x-ray (Cu-kα) reflectivity measurement of a multilayer containing 20 bilayers optimized for the second order reflection of λ=3.374 nm together with a simulation. The simulated intensity is increased 10 times for clarity.

The three major peaks (marked B_1, B_2 and B_3 in the figure) at $2\theta_1$=2.65°, $2\theta_2$=5.22° and $2\theta_3$=7.79° are the first, second and third order multilayer Bragg reflections, respectively, and the positions correspond to a multilayer period of Λ=3.410 nm. Between the Bragg reflections, and all the way up to the third reflection order, very distinct and sharp Kiessig fringes are visible. These oscillations are due to the interference of x-rays that have been reflected from different interfaces. Each peak in the fourier domain is associated with the distance between two interfaces. The number of Kiessig fringes are thus related to the number of bilayers in the multilayer. These regular distances will become irregular if layer thickness variations exists, and thus their highly regular presence is an evidence of a very high layer conformity.

The simulation corresponds very well with the measurement. The discrepancy below the critical angle, $2\theta_C$=0.53°, is due to finite size of the sample, which could not be included in the simulation. At first the x-rays are passing straight into the detector and as the angle increases the x-rays start to be totally reflected from the sample. Because of the limited size of the sample (20 mm) some of the x-rays will pass by the sample and hence not reach the detector, resulting in an intensity loss. As the angle is further increased more of the x-ray beam illuminates the sample and the intensity increases. Above the critical angle all x-rays are incident on the sample.

The simulation yielded individual layer thicknesses of d_{Sc}=2.766 nm and d_{Cr}=0.641 nm, or recalculated, a multilayer period of Λ=3.407 nm and a layer thickness ratio of Γ=0.188. This multilayer period is in very good agreement with the one calculated from the position of the Bragg peaks. The average interface width of the multilayer was determined to 0.962 nm, and on top of that a layer of Cr_2O_3 with a roughness of 1.32 nm.

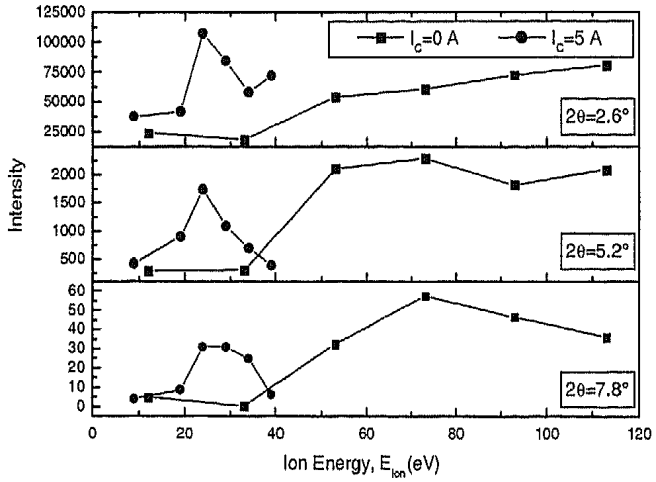

Figure 4: Hard x-ray specular reflectivity of the first three orders of multilayer Bragg reflections as a function of the ion energy for low and high ion fluxes, i.e. solenoid currents of I_C=0 A and 5 A, respectively.

In Figure 4 the intensities of the first three Bragg reflections ($2\theta_1$=2.6°, $2\theta_2$=5.2° and $2\theta_3$=7.8°) are plotted as a function of the ion energy. For the case of low Φ, the first Bragg peak increases for all ion energies. However, the second and third Bragg peaks, which are more roughness sensitive, decrease for energies above 73 eV which indicates that an optimal ion energy exists for obtaining high reflectivity of the mirrors. For the multilayers deposited with a large Φ an optimal ion energy of 24 eV is clearly evident.

Thus, depositing multilayers with varying ion energies resulted in peak shaped behaviours of the x-ray reflectivities for both low and high fluxes of Ar ions. Below the maxima the increase in reflectivities are due to a decrease in interface roughness which can be attributed to an increase in surface mobility, caused by the attracted Ar ions, during the whole deposition of each layer. An increase in surface mobility allows the deposited ad-atoms to move around on the surface and find positions with a local energy minimum, which in turn means a position that smoothens the surface. For a continuing increase in ion energy beyond the reflectivity maxima at 73 eV and 24 eV the observed decreases are due to the knock-on effects of the increasing energy of the Ar ion bombardment, resulting in intermixing of the layer materials. Similar effects have been observed in both amorphous multilayers[15] and single crystal superlattices.[25] Another possible explanation of the decreased reflectivities may be an increasing "waviness" of the layers caused by nucleation of islands. Nucleation of islands may occur if non-wetting conditions apply and if the mobility of ad-atoms is high enough. However, increased waviness would also mean increased interlayer roughness correlation leading to an increased broadening of rocking-scans over the Bragg-peaks.

Rocking-scans were performed (not shown) for three different ion energies, low, optimal and high energy, for each of the two ion fluxes. Decreased rocking curve widths with increasing ion energy for both ion fluxes were observed, showing that the interlayer roughness correlation decreased and thus increased waviness as the cause of decreased reflectivity at higher energies can be excluded.

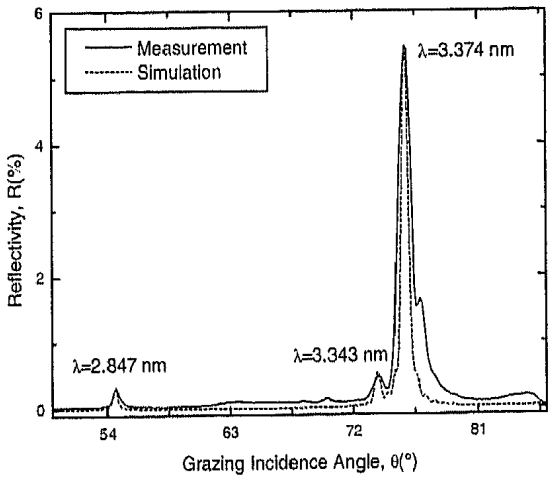

Figure 5: Soft x-ray reflectivity measurement of a multilayer consisting of 400 bilayers optimized for the first order reflection of λ=3.374 nm together with a simulation. Since the soft x-ray source consists of an ethanol target the spectrum contains several wavelengths which are also detected.

Figure 5 shows an at-wavelength (λ=3.374 nm) soft x-ray reflectivity measurement with the highest obtained reflectivity, R=5.47 % at a grazing incidence angle of 76°, for a multilayer deposited with high ion flux and an ion energy of 24 eV. Since the laser-plasma source is using an ethanol target several deexcitation processes takes place and gives rise to other soft x-ray wavelengths. These wavelengths are also reflected by the multilayer and appear in the measured spectrum. Included in the graph is an IMD simulation of the wavelengths λ=2.847 nm, λ=3.343 nm and λ=3.374 nm, all corresponding to carbon deexcitations. To obtain a good fit, first the peak position was obtained by varying the multilayer period for the fix wavelength λ=3.374 nm. Thereafter the simulated reflectivity was decreased to the measured one by increasing the interface width. This resulted in a multilayer period of Λ=1.746 nm and an average interface width of 0.425 nm. In the simulations the layer thickness ratio was fixed to the nominal value, Γ=0.471, and since the first order reflectivity does not vary much with Γ, a small error in Γ should not significantly influence the simulation.

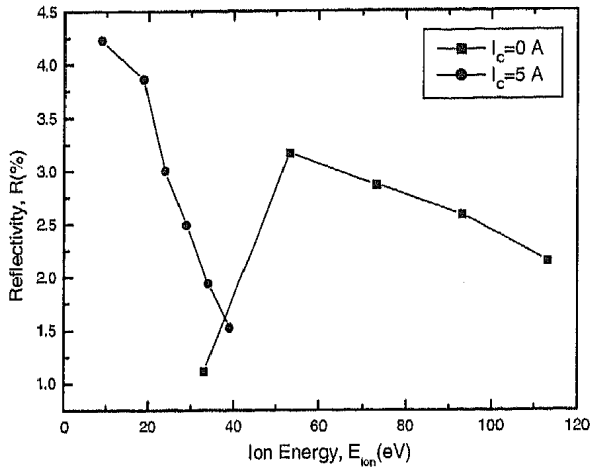

Figure 6: Soft x-ray reflectivity of the first order reflection of λ=3.374 nm as a function of the ion energy for solenoid currents of I_C=0 A and 5 A.

Figure 6 shows the soft x-ray reflectivities of multilayers grown with different ion energies for low and high flux of ions, i.e., I_C=0 A and 5 A, respectively. The multilayers are designed to have the second order reflection of λ=3.374 nm at near-normal incidence, and this figure is showing the first order reflection which appears at a grazing incidence angle close to 30°.

Again the reflectivity shows a peak shaped behaviour for the case of low Ar flux, but now with a maximum for an ion energy of about 53 eV. The reflectivity for the high Ar flux has its highest value for 9 eV corresponding to growth with the sample at floating potential. Although this is not confirmed to be an optimum it is not expected that a lower bias voltage, which causes predominantly electron bombardment instead of ion bombardment, will improve the reflectivity further. A substrate bias potential above the floating potential will quickly produce electron currents up to several orders higher than the ion currents, thus causing resistive heating of the sample with a possible increase of the bulk diffusivities as a consequence.

The reason for these reflectivity behaviours follow the same arguments as given above for the hard x-ray reflectivities. The increase in reflectivity is due to the decreased roughness and then after a certain ion energy the intermixing takes over and the reflectivity decreases. Noteable is the much higher maximal absolute reflectivity that occur already for 9 eV ions using high flux conditions.

As can be seen from the Figures 4 and 6 the maximum reflectivities does not occur at the same ion energies for hard x-rays and soft x-rays. For the high ion flux the soft x-ray maximum occurs at a low ion energy, about 9 eV versus 24 eV in the case of hard x-rays. For low ion flux, the soft and hard x-ray reflectivity maxima appear at and about 53 eV and 73 eV, respectively. The difference is due to the fact that the reflectivity of hard x-rays, which have a wavelength on the atomic scale, is sensitive to roughness down to atomic scale, sometimes referred to as "jaggedness".[26] Soft x-rays, on the other hand, have a wavelength that is 20 times longer and the soft x-ray reflectivity is thus less sensitive to roughness on the atomic scale, but very sensitive to longer spatial frequencies, sometimes called "waviness". The reason for the different positions of the maxima using the two x-ray wavelengths must be that as the ion energy is increased first the waviness is reduced, resulting in an optimum for soft x-rays, and after a further increase of the ion energy the jaggedness is eliminated. During the whole process of increasing the ion energy the intermixing increases.

Although, hard x-ray reflectivity is a very useful tool to obtain the multilayer period, individual layer thicknesses and interface widths, it can be concluded that the optimal deposition parameters must be determined using the actual wavelength for which the multilayer mirror is intended.

4. CONCLUDING REMARKS

As can be seen in Figure 6 the reflectivity of the multilayer deposited with a high density of low energy Ar bombardment is substantially higher than the one deposited with a relatively low density of high energy bombardment. From the discussion above it is clear that this improvement is because of a reduced intermixing (low energy bombardment) and a subsistent surface mobility, owing to the high ion flux, that minimizes the waviness.

From the hard x-ray peak reflectivity data we conclude that a higher ion energy is required to reduce the jaggedness than it is to reduce the waviness. From the above we can conclude that a high density (7.1 and 23.1 ions/metal atom for Cr and Sc, respectively) of low energy (9 eV) Ar ions minimizes the intermixing, while the smoothening effect is still

present. These conditions can not be obtained in ordinary magnetron sputtering setups, which typically yields a low density of high energy ions. These findings are also important in other areas of thin film depositions, such as epitaxy, deposition on semiconductor surfaces, or on temperature sensitive surfaces, where creation of surface defects must be avoided or the bulk temperature must be kept at a minimum.

ACKNOWLEDGMENTS

The authors are grateful to E. M. Gullikson for his help and support in facilitating the soft x-ray absolute reflectivity measurements made at Calibration and standards beamline 6.3.2 at the ALS of the multilayer mirror which was used as a calibration standard.

REFERENCES

1. M. Berglund, L. Rymell, M. Peuker, T. Wilhein, and H. M. Hertz, "Compact Water-Window Transmission X-ray Microscopy", *Journal of Microscopy* **197**, 268-273, 2000
2. H. M. Hertz, M. Berglund, G. A. Johansson, M. Peuker, T. Wilhein, and H. Brismar, "Compact water-window x-ray microscopy with a droplet laser-plasma source", *X-ray Microscopy*, 721, Eds. W. Mayer-Ilse, T. Warwick, and D. Attwood, American Inst. of Physics, 2000
3. A. B. C. Walker, Jr., T. W. Barbee, Jr., R. B. Hoover, J. F. Lindblom, "Soft X-ray Images of the Solar Corona with a Normal-Incidence Cassegrain Multilayer Telescope", *Science* **241**, 1781-1787, 1988
4. E. Spiller, D. G. Stearns, M. Krumrey, "Multilayer x-ray mirrors: Interfacial roughness, scattering, and image quality", *J. Appl. Phys.* **74**, 107-118, 1993
5. D. G. Stearns, R. S. Rosen, and S. P. Vernon, "Multilayer mirror technology for soft x-ray projection lithography", *Applied Optics* **32**, 6952-6960, 1993
6. A. Grudsky, and A. Rudnev, "New possibilities in X-ray microanalysis of nitrogen and oxygen with the application of special types of multilayers", *Optics and Microanalysis 1992*, p.95-8, Proceedings of the Thirteenth International Congress. IOP, Bristol, UK, 1993
7. H. M. Hertz, L. Rymell, M. Berglund, G. A. Johansson, T. Wilhein, Y. Platonov, and D. Broadway, "Normal-incidence condenser mirror arrangement for compact water-window X-ray microscopy", *X-ray Optics, Instruments, and Missions II, SPIE Annual Meeting, Proc. SPIE* **3766**, 247, 1999
8. D. E. Savage, J. Kleiner, N. Schimke, Y.-H. Phang, T. Jankowski, J. Jacobs, R. Kariotis, and M. G. Lagally, "Determination of roughness correlations in multilayer films for x-ray mirrors", *J. Appl. Phys.* **69**, 1411-1424, 1991
9. D. L. Windt, R. Hull, and W. K. Waswkiewicz, "Interface imperfections in metal/Si multilayers", J. Appl. Phys. **71**, 2675-2678, 1992
10. C. C. Walton, G. Thomas, and J. B. Kortright, "X-ray optical multilayers: Microstructure limits on reflectivity at ultra-short periods", *Acta mater.* **46**, 3767-3775, 1998
11. S. S. Andreev, S. R. Müller, Yu. Ya. Platonov, N. I. Polushkin, N. N. Salashchenko, F. Schäfers, S. I. Shinkarev, D. M. Simanovsky, S. Yu. Zuev, "Small d-spacing multilayer structures for the photon energy range E>0.3 keV", SPIE Superintense Laser Fields **1800**, 195-208, 1991
12. Eric E. Fullerton, Ivan K. Schuller, and Y. Bruynseraede, "Quantitative X-ray Diffraction From Superlattices", *MRS-bulletin* **XVII**, No. 12, 33-38, 1992
13. H.-J. Voorma, E. Louis, N. B. Koster, and F. Bijkerk, "Temperature induced diffusion in Mo/Si multilayer mirrors", *J. Appl. Phys.* **83**, No. 9, 4700-4708, 1998
14. J. Birch, Y. Yamamoto, L. Hultman, G. Radnoczi, J.-E. Sundgren, and L. R. Wallenberg, "Growth and structural characterization of single-crystal (001) oriented Mo-V superlattices", *Vacuum* **41**, 1231-1233, 1990
15. K. Järrendahl, J. Birch, L. Hultman, L. R. Wallenberg, G. Radnoczi, H. Arwin, and J.-E. Sundgren, "Growth of Ge/Si Amorphous Superlattices bu Dual-Target DC Magnetron Sputtering", *Mat. Res. Soc. Symp. Proc.***258**, 571-575 1992
16. S. P. Vernon, D. G. Stearns, and R. S. Rosen, "Ion-assisted sputter deposition of molybdenum-silicon multilayers", *Appl. Opt.***32**, no. 34, 6969-6974, 1993
17. E. J. Puik, M. J. van der Wiel, H. Zeijlemaker and J. Verhoeven, "Ion etching of thin W layers: enhanced reflectivity of W-C multilayer coatings", *Appl. Surf. Sci.* **47**, 63-76, 1991
18. E. Spiller, "Smoothening of multilayer x-ray mirrors by ion polishing", *Appl. Phys. Lett.* **54**, 2293-2295, 1989
19. G. Håkansson, J. Birch, L. Hultman, I. P. Ivanov, J.-E. Sundgren, and L. R. Wallenberg, "Ion irradiation effects during growth of Mo/V(001) superlattices by dual-target magnetron sputtering", *Journal of Crystal Growth* **121**, 399-412, 1992
20. J. M. Schneider, S. Rohde, W. D. Sproul, and A. Matthews, "Recent developments in plasma assisted physical vapour deposition", *J. Appl. D: Appl. Phys.* **33**, 173-186, 2000

21. E.B. Svedberg, J. Birch, C.N.L. Edvardsson and J.-E. Sundgren, "Real Time Measurements of Surface Growth Evolution in Magnetron Sputtered Single Crystal Mo/V Superlattices using *in situ* RHEED Analysis", *Surface Science* **431**, 16-25, 1999
22. C.Engström, T. Berlind, J. Birch, L. Hultman, I.P. Ivanov, S.R. Kirkpatrick and S. Rohde, "Design, Plasma Studies, and Ion Assisted Thin Film Growth in an Unbalanced Dual Target Magnetron Sputtering System with a Solenoid", *Vacuum* **56**, 107-113, 2000
23. G. A. Johansson, M. Berglund, F. Eriksson, J. Birch, H. M. Hertz, "Compact soft x-ray reflectometer based on a line-emitting laser-plasma source", *Rev. of Sci. Inst.***72**, 58-62, 2001
24. D. L. Windt, "IMD: Software for modeling the optical properties of multilayer films", *Computers in Physics* **12**, 360-370, 1998
25. E. B. Svedberg, J. Birch, I. Ivanov, E. P. Münger, and J.-E. Sundgren, "Asymmetric interface broadening in epitaxial Mo/W (001) superlattices grown by magnetron sputtering", *J. Vac. Sci. Technol. A.* **16**, 633-638, 1998
26. D. K. G. Boer, A. J. G. Leenaers, "Probing interface roughness by x-ray scattering", *Physica B* **221**, 18-26, 1996